

# A study on air–sea exchange processes and conserved variable analysis over the Indian Ocean with INDOEX IFP-99 data

N. V. Sam, U. C. Mohanty\*, A. N. V. Satyanarayana and P. V. S. Raju

Centre for Atmospheric Sciences, Indian Institute of Technology, New Delhi 110 016, India

**The exchange properties across the Marine Boundary Layer influence atmospheric convection and determine to a large extent the atmospheric circulation in the tropics. In view of these phenomena, an analysis of the surface parameters such as sea–surface temperature, air temperature, wind speed, moisture and cloud cover along the ORV *Sagar Kanya* and *Ronald H. Brown* cruise track was carried out. An attempt was made to examine the changes in these parameters while the ship was passing across the ITCZ region. The humidity was found to be considerably high over the ITCZ than non-ITCZ regions.**

The air–sea interaction processes were studied by computing the radiation fluxes (short-wave and long-wave) and the turbulent heat fluxes (sensible heat and latent heat) using semi-empirical models. Over ITCZ region a net heat loss was found which can be attributed to large convergence, strong convective activity and dense cloud cover, leading to drastic reduction in short-wave radiation. Latitudinal and longitudinal variation of surface meteorological parameters and turbulent fluxes were studied to establish a link with the prevailing convective and clear weather regimes along the cruise tracks.

A conserved variable analysis of the conserved variable such as potential temperature, virtual potential temperature, saturation equivalent potential temperature and specific humidity is carried out at every point of upper air observation from *Ronald H. Brown*. The values are estimated up to a maximum of 3 km to cover the boundary layer. In the ITCZ region due to the convective mixing deeper boundary layers are formed, where a double structure is observed. The Marine Boundary Layer Height is also estimated using thermodynamic profiles.

INDOEX, a cooperative program involving scientists from the United States, Europe, India and Maldives, has many objectives. The major objective is to study the transport of air masses from the land into the Inter Tropical Convergence Zone (ITCZ). ITCZ is the region where the trades meet and it is also a region where the convective

activity is dominant. The atmospheric Marine Boundary Layer (MBL) in turn influences the atmospheric circulation in the tropics. The Convective Boundary Layer (CBL) over the oceans plays a very crucial role in the air–sea exchange of momentum, heat and moisture.

Some regional scale phenomena such as the air–sea interaction processes, low-level temperature inversion and cross-equatorial fluxes of heat and moisture play a significant role in the maintenance of monsoon activity. A few studies in this regard were done during International Indian Ocean Expedition (IIOE) 1963–1965, Indo-Soviet Monsoon Experiment (ISMEX) 1973, and Monsoon Experiment (MONEX) 1979. Bunker<sup>1</sup> discussed the characteristics of surface marine boundary layer using the data from IIOE. Jambunathan and Ramamurty<sup>2</sup> studied the air–sea temperature distribution over the West Indian Ocean. Ramanathan<sup>3</sup> assessed the bulk layer variation over the Arabian Sea along 10°N and along the equator. Pant<sup>4</sup> discussed the vertical structure of the marine boundary layer in the West Indian Ocean using ISMEX data sets. Mohanty and Dube<sup>5</sup> studied the statistical structure of the meteorological parameters over the Bay of Bengal. All these studies illustrate that air–sea exchange processes do play an important role in the energy transport from ocean surface to the atmosphere which in turn act as a feedback mechanism for convection and circulation in the tropics.

The aim of this paper is to analyse the observed surface meteorological parameters along both ORV *Sagar Kanya* and *Ronald H. Brown* cruise tracks as they pass over ITCZ and non-ITCZ regimes. The ITCZ and its influence on the oceanic heat budget is also one of our prime objectives. The global climate depends on the transports mentioned earlier and increasing attention is being given to the parameterization of CBL in global forecast models<sup>6–8</sup>. In an attempt to study the CBL along the cruise track of *Ronald H. Brown*, Conserved Variable Analysis (CVA) was carried out<sup>9</sup>.

## Data

Surface meteorological parameters such as wind speed, wind direction, cloud-cover, sea-level pressure, sea surface temperature (SST), dry-bulb and wet-bulb tempera-

\*For correspondence. (e-mail: mohanty@cas.iitd.ernet.in)

ture were collected every one and half hours on board ORV *Sagar Kanya* (21 January to 10 February) from Goa to Mauritius and every 3 h (18 February to 10 March) from Mauritius to Goa (see figure 1 of Introductory Note). These parameters were collected six hourly on-board *Ronald H. Brown* from 22 February to 30 March (Mauritius to Maldives, (see figure 1 of Satayanaryana *et al.*, this issue). The upper air observations obtained on *Ronald H. Brown* were used for the CVA. Three periods were classified for this study, viz. 24–26 February, 8–12 March and 20–22 March 1999.

**Synoptic condition**

The important synoptic features observed during both the cruises are described in various legs, viz. leg-1, leg-2, leg-3 respectively of ORV *Sagar Kanya* and leg-1, leg-2, leg-3a, leg-3b of *Ronald H. Brown*.

The leg-1 of ORV *Sagar Kanya* was from 21 January 1999 (15°N, 72.3°E) to 4 February 1999 (20°S, 77°E). During the first half of leg-1 (20–29 January), Northern Hemisphere Equatorial Trough (NHET) or ITCZ (N) as well as Southern Hemisphere Equatorial Trough (SHET) or ITCZ (S) existed simultaneously. The ITCZ (S) was continuously active during this period and the belt between equator to 10°S had continuous convective activity. A tropical disturbance was located in the Indian Ocean close to 12°S and 107°E on 22 January 1999. The disturbance moved west south-westwards and on 30 January 1999 it was close to 19.5°S and 83°E and then it gradually weakened. ORV *Sagar Kanya* was close to ITCZ (N) on 25 January 1999 and passed through ITCZ (S) between 28 and 29 January 1999. In the second half of leg-1 (30 January–February 1999), a depression was located on 1 February 1999, close to 12.5°S and

70.5°E which was moving west south-westwards and on 3 February 1999 it was at 19.0°S and 65.0°E. On 5 February 1999 it was found to be close to 22.0°S and 50.5°E. During leg-2 of ORV *Sagar Kanya* (5 February–10 February) when the ship cruised along a constant latitude (20°S) and a varying longitude (76.7°E) significant weather phenomenon was noticed. Leg-3 of ORV *Sagar Kanya* started on 18 February 1999 (19.1°S and 58.9°E) and ended on 10 March (17.4°N and 68.5°E). A relatively calm weather was observed during this leg. However, a tropical disturbance was noticed on 1 March 1999 close to 8.0°S and 92.0°E, that became a depression and later turned to a cyclonic storm on 4 March 1999 (12.5°S and 87.5°E), with intensity T 3.0 (ref. 10). The storm further intensified while moving west-southwestwards and intensified gradually to T 5.0 on 8 March 1999 (near 17.0°S and 67.5°E). This weather phenomenon occurred quite far away from ORV *Sagar Kanya* and therefore no significant influence of the same was noticed along leg-3.

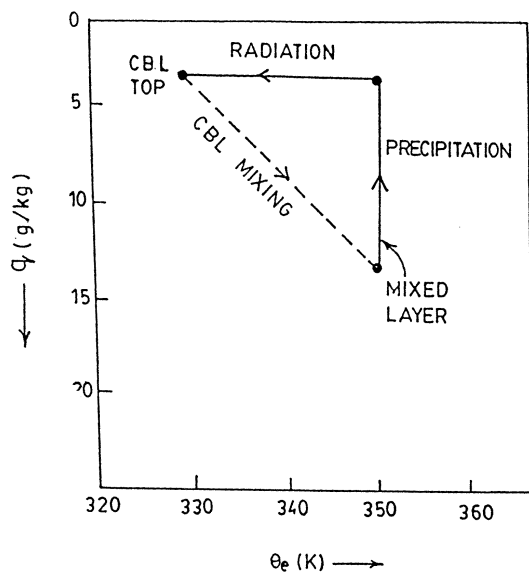


**Figure 1.** An idealized illustration of conserved variable analysis (CVA) (ref. 15).

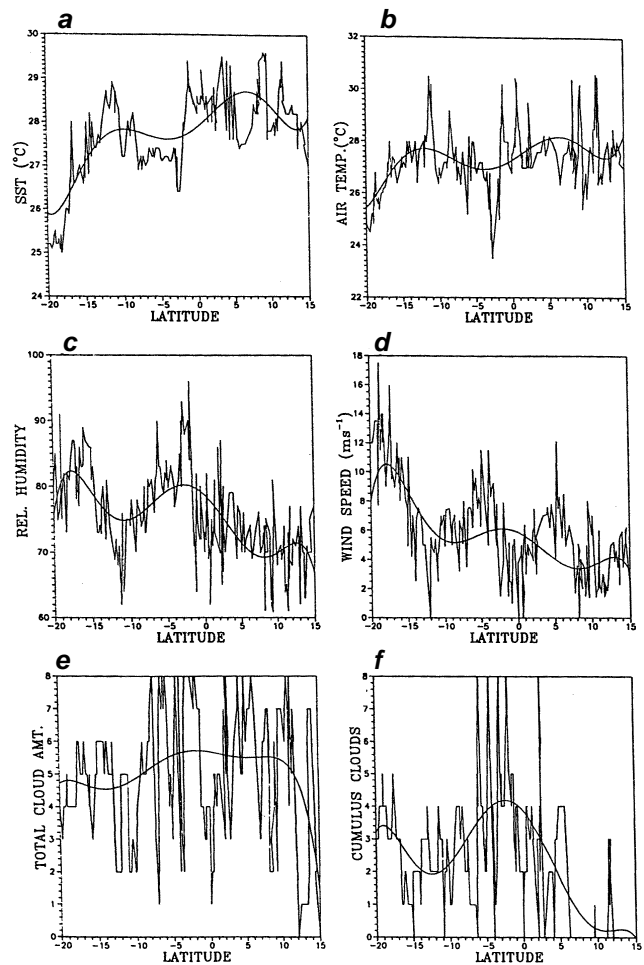


**Figure 2.** Latitudinal variation of observed surface meteorological parameters during leg-1 (21-1-1999 to 4-2-1999) of ORV *Sagar Kanya*. *a*, Sea surface temperature (°C); *b*, Air temperature (°C); *c*, Relative humidity (%); *d*, Wind speed (ms<sup>-1</sup>); *e*, Total cloud amount (octa); *f*, Cumulus clouds (octa).

Leg-1 of *Ronald H. Brown* was from 22 February 1999 (19.0°S, 57.4°E) to 28 February 1999 (2.8°N, 72.1°E). During this period the ship crossed the ITCZ (S). Rain was observed on 23, 24 and 26 February 1999 and the atmosphere found to be convectively active. The sky was overcast with more of cumulus and cumulonimbus clouds during the rainy days. Lightning was observed in the early hours of 28 February 1999. During leg-2 (4 March–10 March 1999) when the ship cruised from 4.7°N and 73.6°E to 18.6°S and 67.5°E, no specific variation in the synoptic parameters was observed. Leg-3a of *Ronald H. Brown* was taken from 11 March 1999 (18.3°N, 67.0°E) to 19 March 1999 (12.3°S, 72.2°E). During the early part of this period, the ship cruised in the Arabian Sea along the western coast of India. A suppressed convection was noticed under the influence of cold and dry continental air from the Indian sub-continent. During the last part of this period (18.5°S to 12°S), the sky was cloudy and rain observed. Leg-3b was from 19 March 1999 (11.9°S, 72.1°E) to the end of the cruise on 30 March 1999

(10.7°N, 85.2°E). Moderate convection was observed between 20 March 1999 (10.6°S, 72.3°E) and 22 March 1999 (2.2°N, 73.7°E) due to a weakened ITCZ. During this period sky was overcast with low clouds and frequent rains were observed.

**Methodology and analysis procedure**

*Surface meteorological parameters*

The parameters such as SST, air temperature, wind speed, moisture and cloud cover are plotted along different legs of both ORV *Sagar Kanya* and *Ronald H. Brown*. The main objective was to see the latitudinal and longitudinal variation of these observed parameters. A linear least-square fit and a polynomial fit were drawn to see the trend of variation in these parameters. Changes observed in the surface synoptic observations during ITCZ and non-ITCZ regimes are linked to the prevailing convective and clear weather regimes along the cruise track.

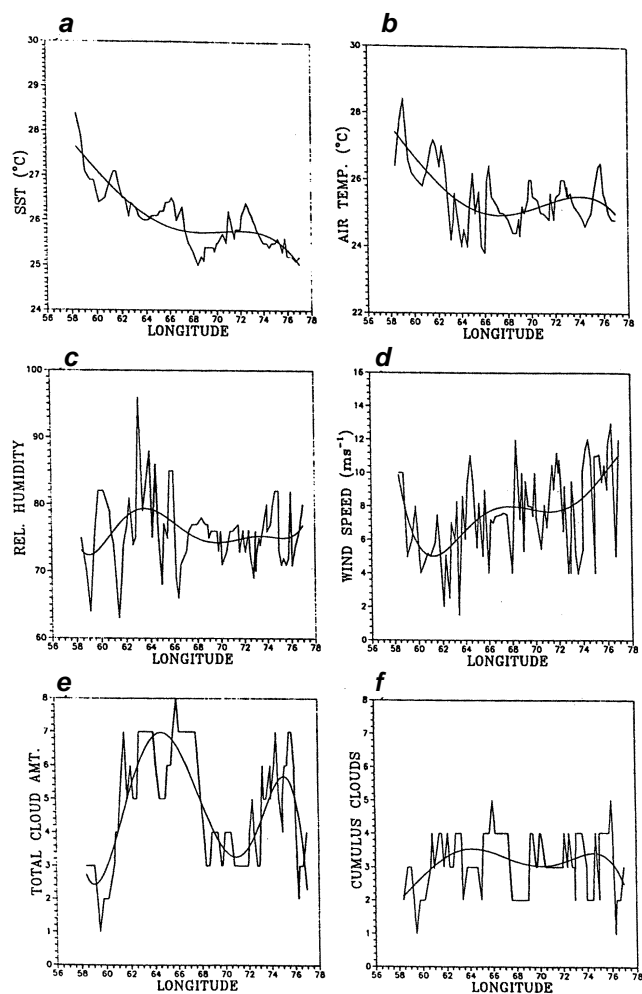


**Figure 3.** Longitudinal variation of observed surface meteorological parameters during leg-2 (5–2–1999 to 10–2–1999) along with polynomial fit for ORV *Sagar Kanya*. *a*, Sea surface temperature (°C); *b*, Air temperature (°C); *c*, Relative humidity (%); *d*, Wind speed ( $m s^{-1}$ ); *e*, Total cloud amount (octa); *f*, Cumulus clouds (octa).

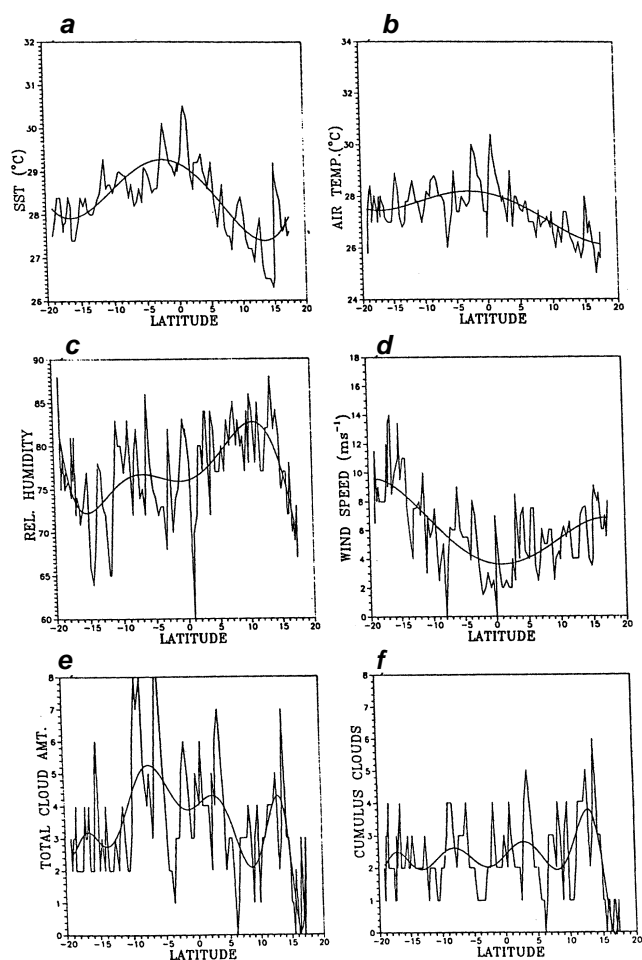


**Figure 4.** Latitudinal variation of observed surface meteorological parameters during leg-3 (18–2–1999 to 10–3–1999) along with polynomial fit for ORV *Sagar Kanya*. *a*, Sea surface temperature (°C); *b*, Air temperature (°C); *c*, Relative humidity (%); *d*, Wind speed ( $m s^{-1}$ ); *e*, Total cloud amount (octa); *f*, Cumulus clouds (octa).

Oceanic heat budget

To study air-sea exchange processes over the Indian Ocean, the radiative fluxes (short-wave and long-wave) and the turbulent heat fluxes (sensible and latent heat) were computed using semi-empirical models and bulk aerodynamic method respectively. The oceanic heat budget equation in  $Wm^{-2}$  can be written as:

$$Q_N = Q_S - Q_B - Q_H - Q_E, \quad (1)$$

where  $Q_N$  is the net heat loss/gain,  $Q_S$  the short-wave radiative flux,  $Q_H$  the sensible heat flux and  $Q_E$  the latent heat flux. Here, the heat transported by ocean currents (advection of heat) is neglected because in short-time scales, it is not appreciable. The parameters on the right-hand side of the equation are computed by the methods suggested by Mohanty and Mohan Kumar<sup>11</sup>.

The short-wave radiation flux reaching the ocean surface was obtained using semi-empirical expression given

by Atwater and Ball<sup>12</sup>, whereas the effective long-wave radiation flux is computed using the expression given by Girduk and Malevaski-Holekyich<sup>13</sup>. The transfer coefficients were computed as a function of both atmospheric stability and wind speed as suggested by Mohanty and Mohan Kumar<sup>14</sup>.

Conserved variable analysis

An idealized illustration of the conserved variable analysis (CVA) is shown in Figure 1 to depict the usefulness of the conserved variable diagram (CVD)<sup>15</sup>. A dashed schematic mixing line<sup>16</sup> is shown between saturation points (SP) of the mixed sub-cloud layer and the CBL top on a  $(q_e, q_T)$  diagram. The  $q_T$ -axis (which becomes  $q$ -axis for unsaturated air) has been reversed so that a sounding data plotted on this diagram superficially resembles a more familiar  $(q_e, p)$  plot. In the absence of irreversible diabatic processes, conserved variables are represented on both the axes.  $q_e$  or  $q_T$  is not changed during condensation

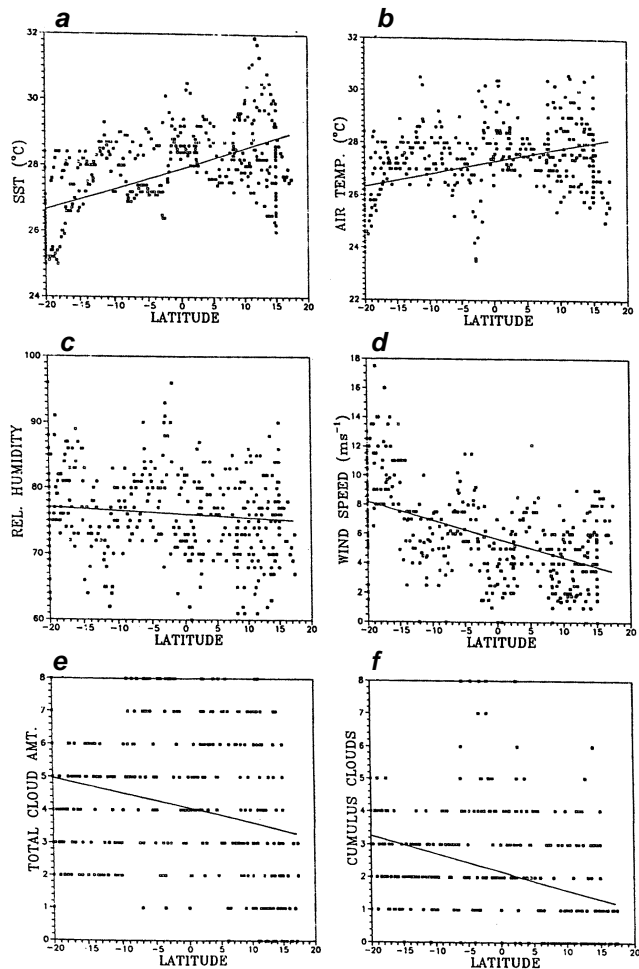


Figure 5. Latitudinal variation of observed surface meteorological parameters during the entire cruise track (21-1-1999 to 10-3-1999) along with linear least-square fit for ORV Sagar Kanya. a, Sea surface temperature ( $^{\circ}C$ ); b, Air temperature ( $^{\circ}C$ ); c, Relative humidity (%); d, Wind speed ( $m s^{-1}$ ); e, Total cloud amount (octa); f, Cumulus clouds (octa).

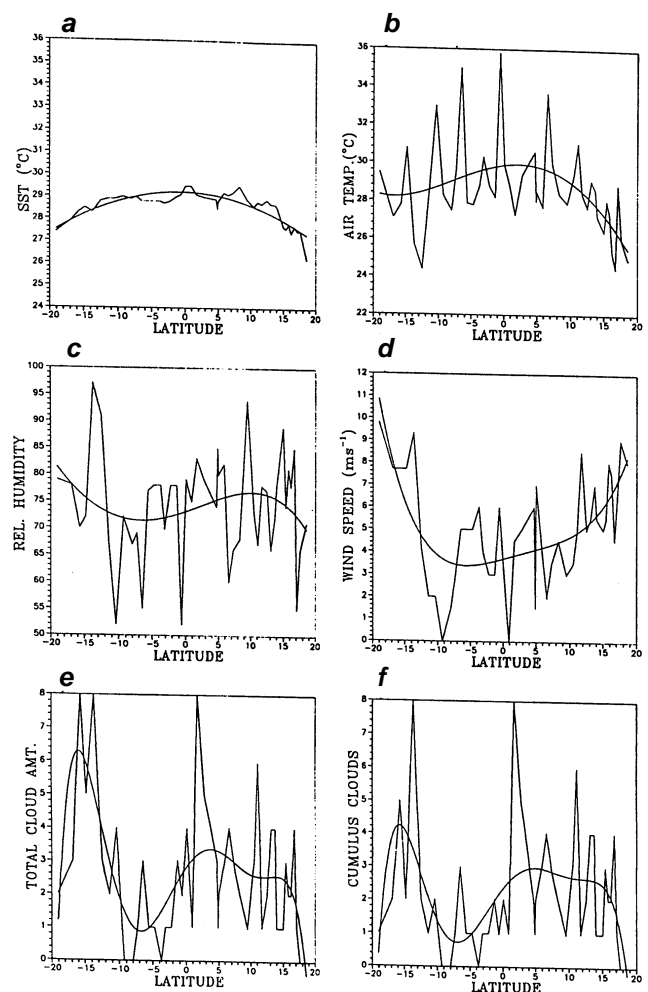


Figure 6. Latitudinal variation of observed surface meteorological parameters during leg-1 (22-1-1999 to 28-3-1999) along with polynomial fit for Ronald H. Brown. a, Sea surface temperature ( $^{\circ}C$ ); b, Air temperature ( $^{\circ}C$ ); c, Relative humidity (%); d, Wind speed ( $m s^{-1}$ ); e, Total cloud amount (octa); f, Cumulus clouds (octa).

process, whereas the precipitating process moves the parcel points to lower  $q_T$  at constant  $q_e$  (and the reverse for the evaporation of falling precipitation). The radiative process does not change  $q_T$ , but radiative cooling moves SP to lower  $q_e$  at constant  $q_T$ . Mixing lines are straight lines and advective processes do not move the parcel points at all. The thermodynamic changes represented by the triangular path show precipitation in the ascending deep convective branch of the tropical circulation which moves the parcel from the sub-cloud layer to lower  $q_T$ , at constant  $q_e$ . Radiative cooling in the subsiding branch lowers  $q_e$  at constant  $q_T$ . The air with the lowest  $q_e$  sinks into the CBL and its SP moves down the mixing line as it is mixed with air from below on its final mean descent back into the sub-cloud layer.

*Marine boundary layer height*

Vertical profiles of virtual potential temperature ( $q_v$ ), equivalent potential temperature ( $q_e$ ) and saturation

equivalent potential temperature ( $q_{es}$ ) are drawn to estimate the marine boundary layer height (MBLH). The MBLH is marked by minimum  $q_e$  and maximum  $q_{es}$ .

**Results and discussion**

The variation of the observed surface meteorological parameters, obtained on board ORV *Sagar Kanya* and *Ronald H. Brown* is represented in Figures 2–5 and Figures 6–8 respectively.

On 28 January 1999 (1.2°S, 77.0°E), the SST (Figure 2 *a*) was observed to be 29.4°C. As the ship entered the ITCZ on 29 January 1999, rain was observed and the sky was overcast with cumulus clouds (Figure 2 *e, f*). The SST dropped to 26.4°C (2.8°S, 77.0°E), while the air temperature (Figure 2 *b*) touched a minimum of 23.5°C. A considerable rise in the relative humidity (Figure 2 *c*) was noticed, which attained a maximum of 96%, just before

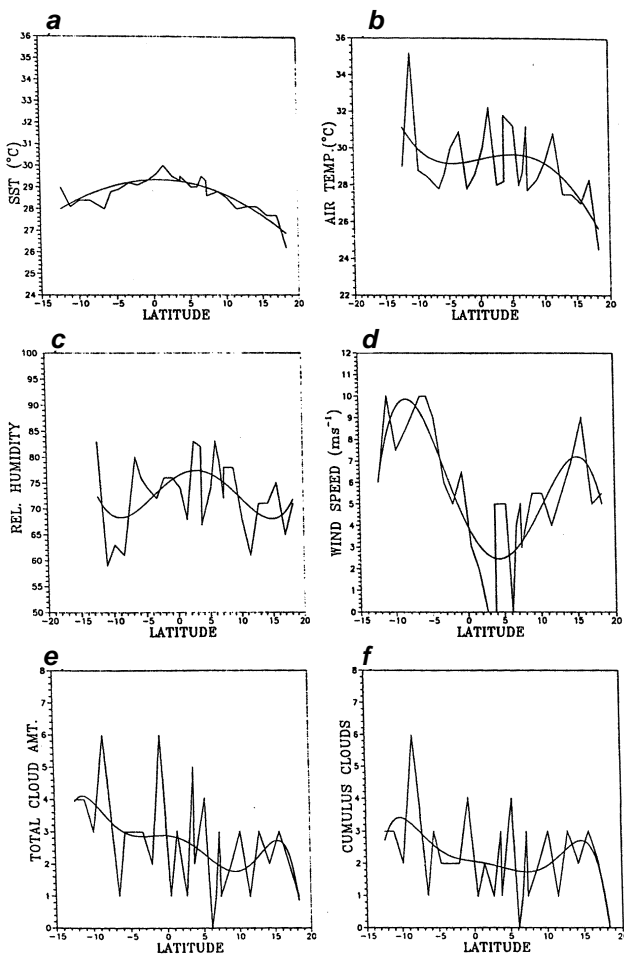


**Figure 7.** Latitudinal variation of observed surface meteorological parameters during leg-2 (4–3–1999 to 10–3–1999) along with polynomial fit for *Ronald H. Brown*. *a*, Sea surface temperature (°C); *b*, Air temperature (°C); *c*, Relative humidity (%); *d*, Wind speed ( $m s^{-1}$ ); *e*, Total cloud amount (octa); *f*, Cumulus clouds (octa).

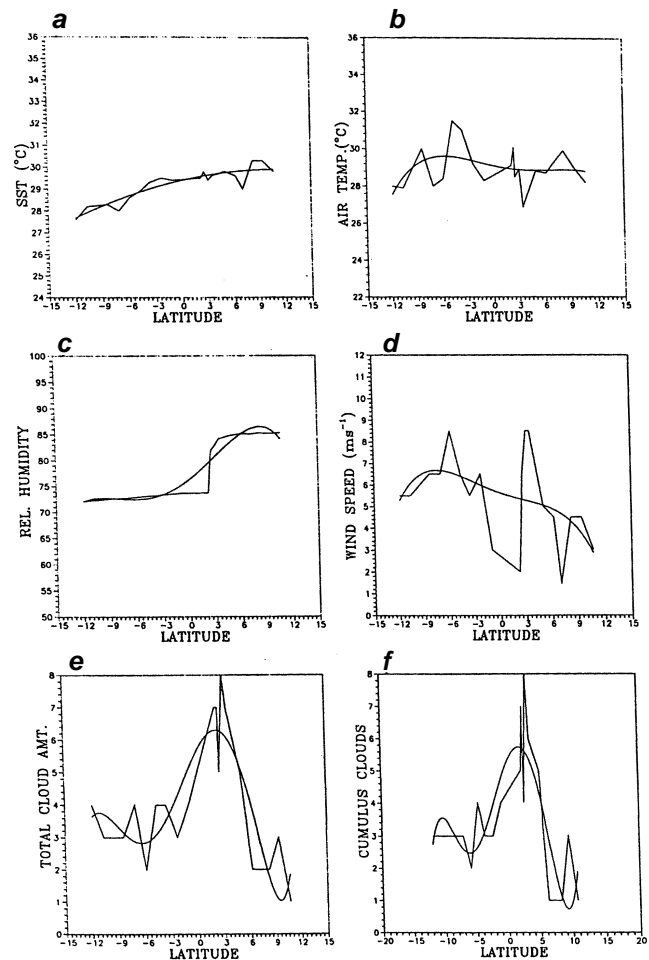


**Figure 8.** Latitudinal variation of observed surface meteorological parameters during leg-3 (11–3–1999 to 19–3–1999) along with polynomial fit for *Ronald H. Brown*. *a*, Sea surface temperature (°C); *b*, Air temperature (°C); *c*, Relative humidity (%); *d*, Wind speed ( $m s^{-1}$ ); *e*, Total cloud amount (octa); *f*, Cumulus clouds (octa).

the rains. The wind speed (Figure 2 d) was found to be low in the ITCZ regime. The wind speed then increased to a maximum of  $11.5 \text{ m s}^{-1}$  soon after crossing the ITCZ and later dipped to a minimum at  $12.1^\circ\text{S}$  and  $77.0^\circ\text{E}$  to rise finally to a maximum of  $17.5 \text{ m s}^{-1}$  ( $18.5^\circ\text{S}$ ,  $77.0^\circ\text{E}$ ). Looking at the latitudinal trend a sea-saw type of variation was noticed in case of SST, air temperature, relative humidity and wind speed. The SST and air temperature showed a general decreasing trend as the ship cruised towards Port Louis ( $20.0^\circ\text{S}$ ,  $58.4^\circ\text{E}$ ). Figure 3 a-f shows the longitudinal variation ( $20^\circ\text{S}$ ,  $77.0^\circ\text{E}$  to  $20^\circ\text{S}$ ,  $58.4^\circ\text{E}$ ) of the surface meteorological parameters. The SST (Figure 3 a) and air temperature (Figure 3 b) show an increasing trend attaining a maximum of  $28.5^\circ\text{C}$  ( $20.0^\circ\text{S}$ ,  $58.4^\circ\text{E}$ ) and  $28.4^\circ\text{C}$  ( $20.0^\circ\text{S}$ ,  $59.1^\circ\text{E}$ ) respectively. No specific variation was noticed in the case of relative humidity (Figure 3 c) and wind speed (Figure 3 d). However, a slow decreasing trend was observed in the case of wind speed with an increase as the ship reaches the coastal waters of Mauritius. The sky was almost overcast (Figure 3 e) between  $67.6^\circ\text{E}$  and  $61.4^\circ\text{E}$ . During this period the relative humidity touched a maximum of 96% ( $20^\circ\text{S}$ ,  $63.1^\circ\text{E}$ ).

The latitudinal variation of the various surface meteorological parameters is given in Figure 4 a-f. Both the SST (Figure 4 a) and the air temperature (Figure 4 b) show an increasing trend towards the equator with a maximum of  $30.5^\circ\text{C}$  ( $1.1^\circ\text{N}$ ,  $63.0^\circ\text{E}$ ) and  $30.4^\circ\text{C}$  ( $0.9^\circ\text{N}$ ,  $63.0^\circ\text{E}$ ) respectively and then gradually decreasing along the course. The polynomial fit depicts this sea-saw change. After an initial decrease from 88% ( $19.1^\circ\text{S}$ ,  $58.9^\circ\text{E}$ ), the relative humidity (Figure 4 c) showed a gradual increase to reach a maximum of 90% ( $15.0^\circ\text{N}$ ,  $62.4^\circ\text{E}$ ) and then it steeply decreases to 67% ( $17.4^\circ\text{N}$ ,  $68.5^\circ\text{E}$ ). Near the equator ( $0.9^\circ\text{N}$ ,  $63.0^\circ\text{E}$ ), the relative humidity touched a minimum of 60%. During this leg, the wind speed (Figure 4 d) decreased from a maximum of  $9.6 \text{ m s}^{-1}$  to minimum values ranging from 0 to  $2.5 \text{ m s}^{-1}$  near the equator and then started increasing gradually as the ship cruised towards Goa. No specific trend was observed in the variation of the cloud amount (Figure 4 e, f), but the sky was overcast between  $10^\circ\text{S}$  and  $5^\circ\text{S}$ . In leg-3 the ship did not encounter the ITCZ and therefore, no specific influence of the same was noticed in the variation of the observed surface parameters.

A linear least-square fit was drawn to see the general trend of the latitudinal variation of the surface meteorological parameters. The SST (Figure 5 a) and the air temperature (Figure 5 b) show a decreasing trend from North to South latitude, implying that the sea is warmer in the Northern Hemisphere. The wind speed (Figure 5 d) was higher in the Southern Hemisphere, while the relative humidity (Figure 5 c) was found to be balanced. The sky was more cloudy (Figure 5 e, f) in the Southern Hemisphere and could be attributed to the active presence of the ITCZ (S).

Changes in the surface synoptic observed parameters during leg-1 of *Ronald H. Brown* are given in Figure 6 a-f. In case of SST (Figure 6 a), no significant variation was observed, while the air temperature rose to a maximum of  $38.5^\circ\text{C}$  at the equator to decrease gradually as the vessel cruised away in the northward direction from the equator. The relative humidity (Figure 6 c) was maximum (98%) at  $13.0^\circ\text{S}$  and  $59.0^\circ\text{E}$ . At the same location the sky was overcast (Figure 6 e) with the dominance of cumulus clouds (Figure 6 f). During this period, rain was observed and a steep decrease in the wind speed (Figure 6 d) noticed. The influence of the ITCZ (S) was quite evident with the changes observed in the surface synoptic parameters.

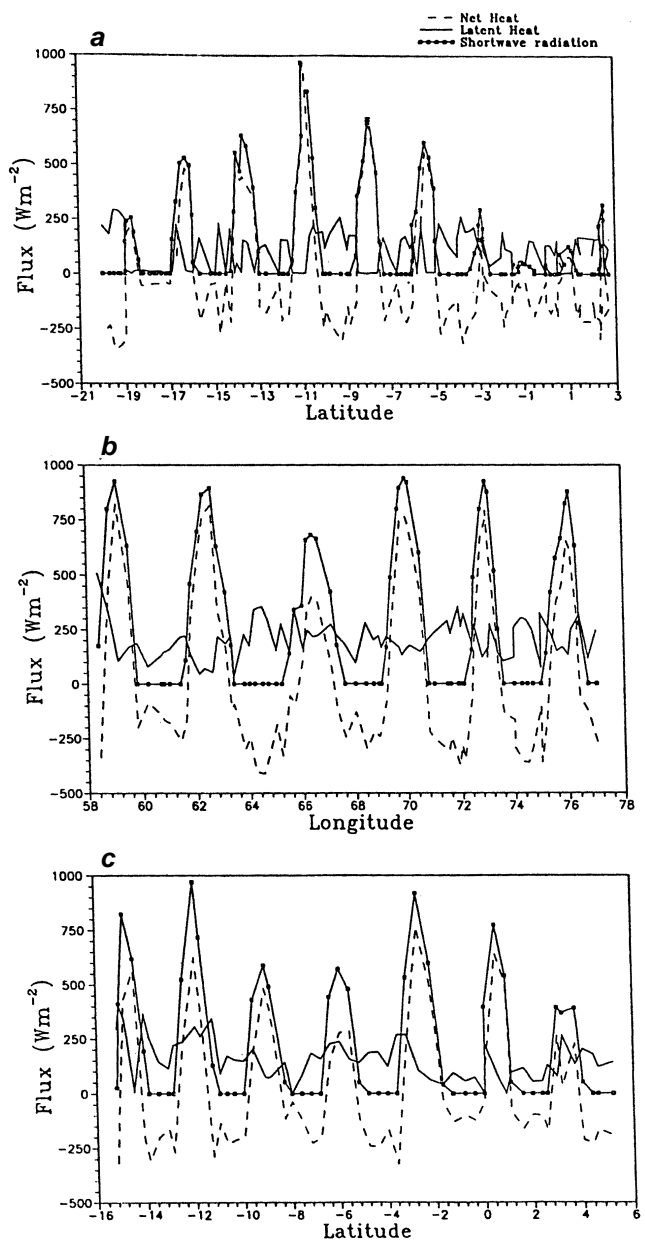


Figure 9. Variation of oceanic heat budget components during leg-1 (a), leg-2 (b) and leg-3 (c) of ORV *Sagar Kanya*.

## INDIAN OCEAN EXPERIMENT

The SST (Figure 7 *a*) was maximum at 29.5°C near the equator (0.5°N, 75.0°E) during leg-2 and leg-3a of *Ronald H. Brown*, while the air temperature (Figure 7 *b*) rose to a maximum of 35.8°C (11.0°S, 72.6°E). No significant variation was seen in case of relative humidity (Figure 7 *c*) except that it touched a low of 58% near 12°S. However, the wind speed (Figure 7 *d*) depicted a sea-saw change with minimum (0–4 m s<sup>-1</sup>) near the equator and maximum of 7.5 m s<sup>-1</sup> (4.9°N, 73.4°E) and 10 m s<sup>-1</sup> (6.5°S, 73.2°E) at the north and south latitude respectively. The sky was partially cloudy towards the end of leg-3a and rain was also observed during this period.

In leg-3b (Figure 8 *a–f*), a gradual increasing trend of SST (Figure 8 *a*) was observed as the ship moved from south to north latitude. No specific variation was noticed in case of air-temperature (Figure 8 *b*), except that a maximum of 31.5°C (4.7°N, 73.1°E) was recorded just before passing through the weakened ITCZ (S). The relative humidity (Figure 8 *c*) rose sharply at around 2°S and 73.7°E. At the same location, the sky was overcast with cumulus clouds. The wind speed (Figure 8 *d*) had an overall decreasing trend from south to north latitude.

The various components of the oceanic heat budget (daily variation) are computed using the surface synoptic observations. Since the contribution to the net heat ( $Q_N$ ) was dominated by the short-wave radiation flux ( $Q_S$ ) and latent heat flux ( $Q_E$ ), the long-wave radiation flux ( $Q_B$ ) and the sensible heat flux ( $Q_H$ ) are not shown in Figure 9 *a–c* and Figure 10 *a–d* for clarity.

Figure 9 *a–c* gives the oceanic heat budget along the cruise track of ORV *Sagar Kanya*. The incoming solar radiation was near zero as the vessel cruised from 3°N to 3°S (Figure 9 *a*). A net oceanic heat loss was seen during this period. The presence of the convectively active ITCZ and its influence on the oceanic heat budget parameters are reflected by the net oceanic heat loss. Between 28 and 29 January 1999, when the ship passed through the ITCZ, the net heat loss was 109 Wm<sup>-2</sup>. During this leg the maximum  $Q_E$  ranged from 150 to 300 Wm<sup>-2</sup>. At around 11.5°S latitude the solar radiation reached a maximum of 1000 Wm<sup>-2</sup>. There was a significant increase of latent heat flux even during day due to the strong convection (ITCZ) and its influence was noticed up to 5°S along this leg. Therefore, it may be inferred that oceanic heat loss produces a positive feedback for the maintenance and development of cumulus convection in the troposphere<sup>11</sup>. This fact is well known from the daily variation of the components of the oceanic heat budget. The sensible heat flux and the long-wave radiation flux were of the order of 10 Wm<sup>-2</sup> and 35 Wm<sup>-2</sup> respectively, throughout the cruise.

No specific trend was noticed in case of the longitudinal (Figure 9 *b*) variation of the oceanic heat budget parameters (leg-2). In this leg the solar radiation was of the order of 750–950 Wm<sup>-2</sup>. There was a considerable increase in the latent heat flux compared with the previous leg, which reaches to a maximum of 500 Wm<sup>-2</sup> as the vessel was near Port Louis (20°S, 58.4°E). Larger surface

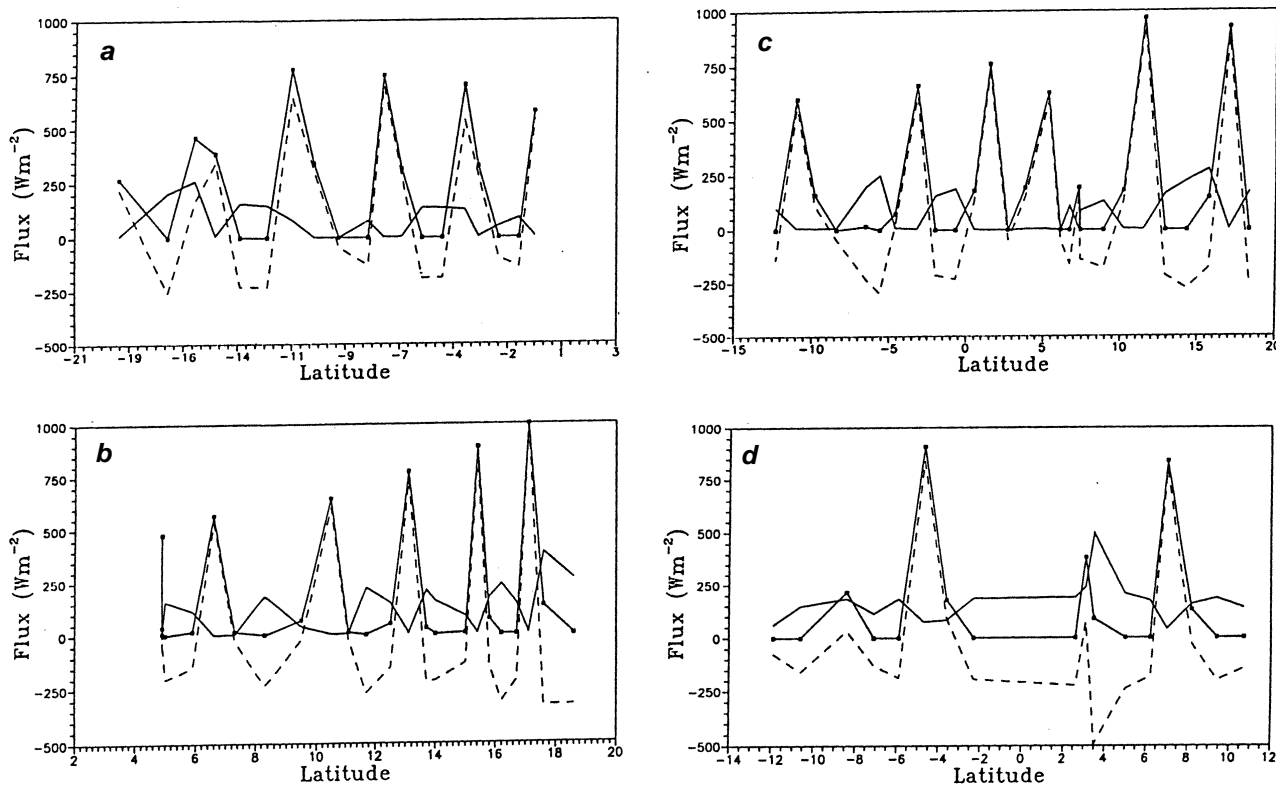


Figure 10. Variation of oceanic heat budget components during leg-1 (*a*), leg-2 (*b*), leg-3a (*c*) and leg-3b (*d*) of *Ronald H. Brown*.

**Table 1.** Mean of the different components of the oceanic heat budget during different legs of ORV *Sagar Kanya* and *Ronald H. Brown*

Legs	From	To	$Q_S$	$Q_B$	$Q_H$	$Q_E$	$Q_N$
<i>(a) Sagar Kanya</i>							
Leg-1	21 January (15.0°N, 72.3°E)	4 February (20.0°S, 77.0°E)	137.78	36.55	5.29	89.90	6.03
Leg-2	5 February (20.0°S, 76.7°E)	10 February (20.0°S, 58.4°E)	304.39	31.30	4.65	204.67	63.74
Leg-3	18 February (19.1°S, 58.9°E)	10 February (17.4°N, 68.5°E)	224.39	40.00	9.07	157.17	18.14
<i>(b) Ronald H. Brown</i>							
Leg-1	22 January (19.0°S, 57.4°E)	22 January (2.8°N, 72.4°N)	258.28	39.75	6.65	78.98	132.90
Leg-2	4 March (4.7°N, 73.6°E)	10 March (18.6°N, 67.5°E)	199.30	42.01	7.76	108.72	42.82
Leg-3a	11 March (18.3°N, 67.0°E)	19 March (12.3°S, 72.0°E)	209.91	39.75	4.83	71.78	103.33
Leg-3b	19 March (11.9°S, 72.1°E)	30 March (10.7°N, 85.2°E)	148.53	36.94	9.42	146.06	- 1.96

winds ( $8-13 \text{ m s}^{-1}$ ) could be one of the reasons for the higher values of  $Q_H$ . On the return journey of ORV *Sagar Kanya* (leg-3) from Port Louis to Goa (Figure 9 c), the solar radiation flux dominated. The latent heat flux was higher in leg-3. Table 1 a gives the mean of the various oceanic heat budget parameters along the different legs of ORV *Sagar Kanya*.

Figure 10 a-d shows  $Q_S$ ,  $Q_H$  and  $Q_N$  computed from the surface synoptic observations obtained on board *Ronald H. Brown*. The influence of the ITCZ (S) was noticed as the ship cruised from  $16^\circ\text{S}$  to  $12^\circ\text{S}$  latitude (Figure 10 a). The solar radiation was reduced considerably and the latent heat flux rose to a maximum of  $265 \text{ W m}^{-2}$ . During this period the wind speed was  $7-9 \text{ m s}^{-1}$ . During leg-2 (Figure 10 b), a gradual increase in the solar radiation flux was noticed, which reached a maximum of  $1000 \text{ W m}^{-2}$  at  $17.6^\circ\text{N}$  and  $69.3^\circ\text{E}$ . As such no significant trend was noticed in this leg. Much influence of the weakened ITCZ was not felt on the net oceanic heat budget during leg-3a (Figure 10 c). However, there was a steep decrease of solar radiation, to around  $200 \text{ W m}^{-2}$  at  $7^\circ\text{N}$  and  $71.7^\circ\text{E}$ , which could be due to partial cloudiness. The influence of the ITCZ, even though weakened, was felt and can be inferred from Figure 10 d (leg-3b). The solar radiation flux dropped to around  $200 \text{ W m}^{-2}$  ( $8.4^\circ\text{S}$ ,  $72.6^\circ\text{E}$ ) when the vessel passed through the ITCZ regime (20-22 March 1999). Again, on 28 March 1999 ( $3.5^\circ\text{N}$ ,  $84.1^\circ\text{E}$ ), the solar radiation flux dropped to  $400 \text{ W m}^{-2}$ . This could be due to the rains and prevalent cloudy conditions along the cruise track of this leg. Table 1 b gives the mean of both the radiation and surface fluxes. This Table also shows a net oceanic heat loss during this leg.

The  $(q_e, q)$  plots (Figure 11 a-f) show a double mixing line structure with a small reversal at the CBL top. The existence of the double mixing line structure in the ITCZ regime (24-26 February) is difficult to be explained. But

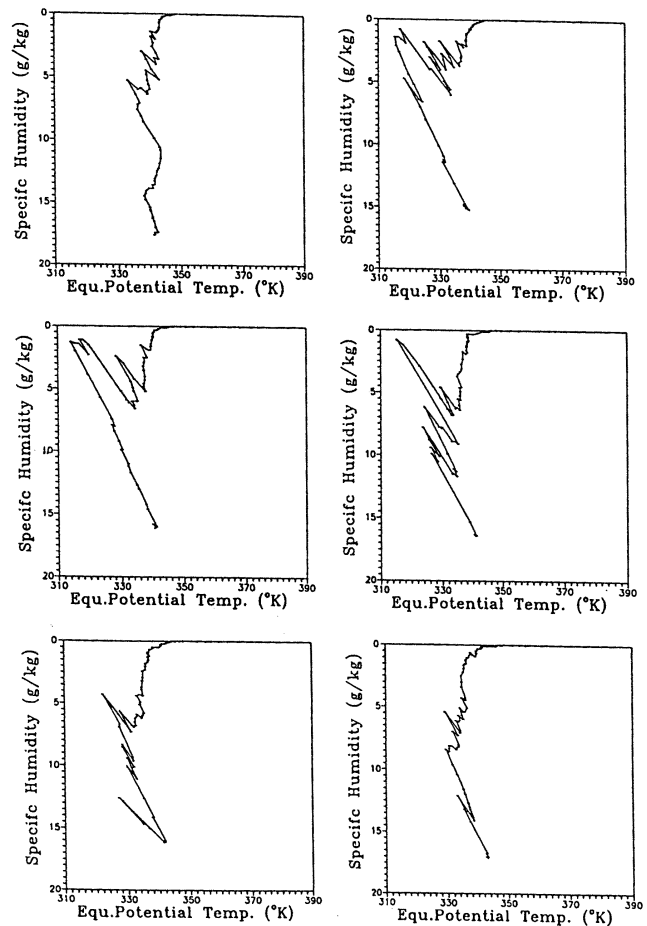


**Figure 11.**  $q_e-q$  profile showing double mixing line structure on 24-26 February 1999 using *Ronald H. Brown* cruise data.

it is speculated that the differential horizontal advection of boundary layer of different depths could be the possibility. These double structures at the top of the CBL involve reversals in  $q_e$  and  $q$  gradients with height. The  $q$



**Table 2.** Marine boundary layer height (m)

Date/Time (IST)	Lat./Long.	MBLH (m)
<b>(a) 24–26 February 1999</b>		
24–2–99/04:30	12.83°S/58.93°E	1400
24–2–99/16:30	10.74°S/59.33°E	1457
25–2–99/22:30	9.55°S/59.53°E	1754
25–2–99/04:30	8.30°S/59.80°E	959
25–2–99/16:30	6.87°S/61.28°E	1253
25–2–99/22:30	5.86°S/61.91°E	888
26–2–99/04:30	4.94°S/62.99°E	874
<b>(b) 8–12 March 1999</b>		
8–3–99/04:30	12.39°N/68.18°E	417
8–3–99/16:30	13.57°N/68.47°E	780
8–3–99/22:30	14.21°N/68.74°E	777
9–3–99/04:30	14.84°N/69.19°E	606
9–3–99/16:30	15.72°N/69.82°E	514
9–3–99/22:30	16.11°N/69.50°E	680
10–3–99/04:30	16.60°N/69.08°E	945
10–3–99/16:30	17.45°N/68.42°E	600
10–3–99/22:30	18.35°N/67.67°E	920
11–3–99/04:30	18.61°N/67.00°E	665
11–3–99/16:30	16.04°N/67.00°E	856
11–3–99/22:30	14.59°N/67.07°E	959
12–3–99/04:30	13.15°N/67.00°E	1137
12–3–99/16:30	10.59°N/66.99°E	856
12–3–99/22:30	9.20°N/67.00°E	1051
<b>(c) 20–22 March 1999</b>		
20–3–99/04:30	8.65°S/72.56°E	1161
20–3–99/10:30	7.41°S/72.72°E	1755
20–3–99/16:30	6.06°S/72.90°E	1549
21–3–99/10:30	4.87°S/73.06°E	1075
21–3–99/16:30	3.93°S/73.19°E	1951
21–3–99/22:30	2.63°S/73.35°E	1352
22–3–99/04:30	1.26°S/73.53°E	1952
22–3–99/10:30	0.12°S/73.65°E	1253
22–3–99/16:30	0.70°S/73.70°E	1549
22–3–99/22:30	1.91°S/73.75°E	1752

minimum was observed at the top of the CBL. A mixed layer structure was produced when the vertical convective mixing dominates over the processes that do not conserve the thermodynamic variables. As suggested by Betts *et al.*, the precipitation–evaporation process is responsible for this double mixed layer structure once the CBL reach a sufficient depth.

Table 2 gives the MBLH at the ITCZ and non-ITCZ regimes along the cruise track of *Ronald H. Brown*. The MBLH was estimated using  $q_e$  and  $q_{es}$  profiles, where the top of the MBL is typically characterized by a maximum in  $q_{es}$  and a minimum in  $q_e$ . Table 2 *a* gives the variation in the MBLH when the vessel passed through the ITCZ (12.5°S, 58.9°E to 2.2°S, 66.2°E) between 24 and 26 February; while Table 2 *c* represents the MBLH variation during the weakened ITCZ (10.6°S, 72.3°E to 2.2°N, 73.7°E). During the non-ITCZ regime we noticed that the MBLH had decreased considerably due to calm weather and lack of any convective activity. The strong convection in the ITCZ region led to the increase in the MBLH here.

The average MBLH in the ITCZ (24–26 February 1999 and 20–22 March 1999) and non-ITCZ (8–12 March 1999) regime was 1226 m, 1554 m and 784 m respectively.

## Conclusions

From the results of the study, the following broad conclusions can be drawn.

- Distinct latitudinal variation was observed in the surface meteorological parameters, which were obtained onboard ORV *Sagar Kanya* and *Ronald H. Brown* at ITCZ and non-ITCZ regimes.
- A net oceanic heat loss of  $109 \text{ Wm}^{-1}$  was seen as ORV *Sagar Kanya* passed through the ITCZ regime.
- Characteristic double mixing line structure was observed in the vicinity of the ITCZ.
- The double mixing line structure could be due to the precipitation–evaporation processes, as rain was observed in that period.

1. Bunker, A. F., Proc. Symp. on Met. Results, IIOE, Bombay, 1965, pp. 3–16.
2. Jambunathan, R. and Ramamurty, K., *Indian J. Meteorol. Geophys.*, 1975, **25**, 377–410.
3. Ramanathan, Y., *Indian J. Meteorol. Geophys.*, 1978, **29**, 643–654.
4. Pant, M. C., *Indian J. Hydrol. Geophys.*, 1978, **29**, 88.
5. Mohanty, U. C. and Dube, S. K., *Mausam*, 1981, **32**, 315–320.
6. Betts, A. K. and Miller, M. J., *Quart. J. R. Meteorol. Soc.*, 1986, **112**, 693–701.
7. Betts, A. K., *Quart. J. R. Meteorol. Soc.*, 1986, **112**, 677–691.
8. Albrecht, B. A., Ramanathan, V. and Boville, B. A., *Royal Meteorol. Society*, 1986, pp. 73–104.
9. Betts, A. K., *J. Atmos. Sci.*, 1985, **42**, 2751–2763.
10. Madan, O. P., Pareek, R. S., Kalasi, S. R. and Mohanty, U. C., Abstract Book of Indoex Workshop–IFP '99, 1999.
11. Mohanty, U. C. and Mohan Kumar, *Atmospheric Environ.*, 1990, **24A**, 823–828.
12. Atwater, M. A. and Ball, J. T., *Mon. Wea. Rev.*, 1981, **109**, 878–888.
13. Girduk, G. V. and Malevaski-Holekyich, S. P., *Trudi Main Geophys. Observ. Leningrad*, 1973, **297**, 124–132.
14. Mohanty, U. C. and Mohan Kumar, *Indian J. Marine Sci.*, 1998, **27**, 60–65.
15. Betts, A. K. and Bruce, A. Albrecht, *J. Atmos. Sci.*, 1987, **44**, 83–99.
16. Betts, A. K., *J. Atmos. Sci.*, 1982, **39**, 1484–1505.

ACKNOWLEDGEMENTS. We thank the India Meteorological Department for providing all the necessary help to carry out surface meteorological observations on board ORV *Sagar Kanya*. We also thank Prof. Sethu Raman and his group for providing the necessary data, obtained on board *Ronald H. Brown* to carry out this work. Our gratitude is also due to CSIR, New Delhi, the Department of Space, Govt of India, the INDOEX-India Programme Directorate, the Naval Research Laboratory and the Office of Naval Research Washington DC, for providing the necessary funds to complete this study.